CTU Journal of Innovation and Sustainable Development
ISSN 2615-9422 | e-ISSN 2815-5602

DOI:10.22144/ctujoisd.2023.054

Study of the activation of Truc Thon ball clay by acids

Ngo Truong Ngoc Mai*, Nguyen Minh Nhut, Cao Luu Ngoc Hanh, Tran Thi Bich Quyen, Nguyen Viet Nhan Hoa, and Tran Nguyen Phuong Lan

College of Engineering, Can Tho University, Viet Nam

**Corresponding author (ntnmai@ctu.edu.vn)*

Article info.

Received 6 Jun 2023
Revised 29 Jun 2023
Accepted 6 Jul 2023

Keywords

Acid activation, activated clay, adsorbents, montmorillonite, treated clay

ABSTRACT

Natural clay minerals have attracted attention for their availability and economical cost as adsorbents in the treatment of contaminants in aquatic environments. In this study, Truc Thon white ball clay from Hai Duong province, Vietnam was activated by different acids including H_2SO_4, HCl and H_3PO_4 at 110°C from 6 to 18 hours under refluxing conditions. The chemical composition and structure changes before and after the activation of the clay were characterized by X-ray fluorescence, X-Ray Diffraction and Fourier transform infrared spectroscopy. The raw clay is mainly composed of minerals containing alumina and silica while in activated clay, silica is dominant in amorphous phase. The specific area of clay particles was increased significantly after acid treatment from 10.55 $m^2.g^{-1}$ to 178.53 $m^2.g^{-1}$. Images from a scanning electron microscope also reveal more porous structure of activated clay. These behaviors make acid activated clay highly effective in various adsorption applications.

1. INTRODUCTION

Ball clay has been widely used for years as an inexpensive and versatile natural material in several industries such as manufacturing ceramic products used in construction, household, paper coating, paint extender, rubber filler, and technical products like refractories and electrical insulators (Edama et al., 2014). White ball clay contains mainly kaolinite $Al_2Si_2O_5(OH)_4$, a layer-structured mineral in which each layer is formed by a $[Si_2O_5]^{2-}$ sheet and a $[Al_2(OH)_4]^{2+}$ sheet bonded together via apical oxygens (Murray, 2006). Because kaolinite originates from the weathering of feldspars, alkalis and alkaline earth such as K_2O, Na_2O, CaO, and MgO may coexist in the clay composition.

The applications of clay can be expanded technically using heat treatment, mechanical activation and chemically functionalized modifications so that treated clays can be used in adsorption, wastewater treatment, gas adsorption, and catalysis for natural oil technology (Akpomie & Dawodu, 2016; David et al., 2020; Ahmadi et al., 2020; Dim & Termtanun, 2021; AlKhafaji et al., 2022). The chemical modifications under acid and alkaline conditions have been applied to several types of clay from different origins (Komadel & Madejová, 2013; Akpomie & Dawodu, 2016; Ndé et al., 2019; David et al., 2020). Acid activation of clay usually results in the loss of metal ions, especially octahedral Al^{3+} cations, and the increase in the amorphous SiO_2 phase, while alkaline activation mainly leads to the formation of zeolite (Belver et al., 2002; Crundwell, 2014). Acid treatment changes the composition and structure of clay because of the dissolution of cations, moreover, the surface area, the porosity and the acid centers of the clay significantly increase. This leads to various applications of acid-activated clay as adsorbents and catalyst supports.

In this study, the acid activation was conducted on white ball clay taken from Truc Thon mine, Hai

Duong province, Vietnam after the calcination at 700°C. Raw clay, calcinated clay, and activated clay were chemically and structurally characterized to analyze the process of activation by different acids. From that, the study will discuss the factors governing the process, including types of acid and activation time and suggest technical applications of activated clay based on its properties.

2. MATERIALS AND METHOD

All chemicals were purchased from Xilong Scientific, including phosphoric acid H_3PO_4 (85%), sulfuric acid H_2SO_4 (98%), and hydrochloric acid HCl (36.5%). Ball clay was taken from Truc Thon, Chi Linh, Hai Duong province.

2.1. Preparation of clay before the activation

Raw ball clay was crushed into powder and passed through a 200-mesh sieve. 100 g of clay powder was calcined at 700°C, 10 h in a Nabertherm chamber furnace. Calcinated clay was ground and sieved again into a fine powder ready for the activation process.

2.2. Activation of clay by various acids

Several studies showed that the acid solution used to activate the clay is quite concentrated (Belver et al., 2002; Akpomie & Dawodu, 2016). This is obvious since the clay mineral structures are well-defined and hard to destroy. In this study, the concentrations of all acid solutions (HCl, H_2SO_4, H_3PO_4) were fixed at 6 M at 110°C under reflux conditions. Weight ratio of clay:acid solution = 1:30 was used. Other ratios with a higher amount of clay were tested but the suspensions (clay and acid) were too thick for the activation reactions to occur.

8 g calcinated clay was added to a 500 mL round flask containing the acid solution. The mixture was heated in refluxing condition at 110°C while magnetic stirring at 400 rpm for 6 h, 12 h, and 18 h. After completion, the mixture was cooled to room temperature and washed several times with distilled water until the pH was neutral. Then, the solid particles were separated by vacuum filtering and dried at 105°C. The solid was then sieved to obtain a fine powder of activated clay.

2.3. Characterization of clay before and after acid activation

2.3.1. Chemical composition

X-ray fluorescence (XRF) spectroscopy on a Horiba MESA-50 model was used to analyze the elemental composition of materials. The data were then calculated to the oxide composition of clay before and after the activation.

2.3.2. Thermal analysis

Thermal gravimetry (TG) and Differential scanning calorimetry (DSC) techniques were implemented in a Simultaneous LABSYS evo TG-DSC 1600°C from Setaram Instrumentation. The measurement was run from room temperature to 1150°C with Pt crucibles in an N_2 atmosphere.

2.3.3. X-ray diffraction (XRD)

The powder XRD patterns were recorded on a D8 Bruker Diffractometer using Cu Kα radiation (λ = 1.5406 Å) at 40 kV with a scanning speed of 0.02°/s over a 2 theta range from 10° to 70°.

2.3.4. Weight loss after activation

The weight loss of each clay sample was calculated for different acid solutions used at different reaction times.

2.3.5. Specific surface area

The measurements of specific surface area were performed on a NOVA 2200e - Surface Area and Pore Size Analyzer, Quantachrome Instruments (USA) by nitrogen adsorption/desorption. The Brunauer–Emmett–Teller (BET) method was used to determine the specific surface areas (S_{BET}) at 77 K in liquid nitrogen.

2.3.6. Scanning electron microscopy (SEM)

The morphology of the samples was analyzed on a field-emission scanning electron microscope (FE-SEM) (Hitachi, S-4800) at an accelerating voltage of 10 kV after gold coating.

2.3.7. Measurement of surface charge

The surface charge of clay predicts its adsorption ability in a solution at various pH through the point of zero charge (pH_{pzc}). 0.2 g of clay was added to 100 mL KCl 0.01 M at pH ranging from 3 to 10 ($pH_{initial}$) and shook for 24h. pH of the solution was then measured again (pH_{final}). Plotting the $\Delta pH = pH_{initial} - pH_{final}$ versus initial pH shows the point where ΔpH is zero at a certain initial pH, called the point of zero charge (pH_{pzc}). At $pH < pH_{pzc}$, clay possesses a positive surface charge and at $pH > pH_{pzc}$, the surface charge of clay is negative.

3. RESULTS AND DISCUSSION

3.1. Characterization of raw ball clay

3.1.1. Thermogravimetric analysis

The thermogravimetric analysis of raw clay is shown in Figure 1. When heating to 1150°C, the total weight loss is 13.13%, mainly because of the loss of water and organic compounds in clay. Between 30 to 364.8°C, only 0.58 wt% is lost, originating from adsorbed water. In the range of 365 to 521°C, some endothermic reactions occur, which can be assigned as the decomposition of organic materials. However, the weight loss is only 1.04%. Significant weight loss occurs between 600 to 800°C with a decrease of about 11.51 wt%. In this range, the binding water in kaolinite and montmorillonite is released, and the clay loses its plasticity (Belver et al., 2002, Parker & Kiricsi, 1995). Above 950°C, various exothermic reactions occurred, corresponding to the formation of new minerals, including spinel, mullite, and cristobalite. These minerals make clay become hard and acquire strength. In this study, the clay was calcined at 700°C in 10 h to remove adsorbed and binding water and became more porous. Hence, the activation in acid solution is facilitated.

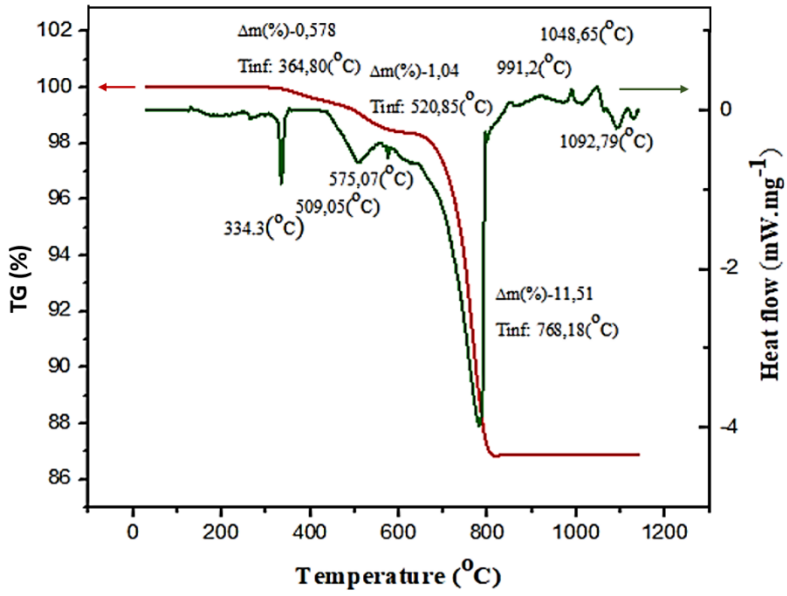

Figure 1. Thermal gravity curve of raw clay

3.1.2. Structural analysis by XRD

The XRD patterns of raw clay and calcinated clay are shown in Figure 2. For the raw clay sample, the main characteristic peaks correspond to the predicted minerals, including kaolinite (at 12.24°; 21.17°; 24.95°; 38.34°; 62.39°), montmorillonite (at 19.8°; 35.26°) and quartz (at 26.67°). Besides, other minor minerals like chlorite (at 17.72°) and illite (at 27.2°; 45.31°) are present (Bhattacharyya& Gupta, 2006). In calcinated clay, the kaolinite peaks almost disappeared because of the decomposition of kaolinite in the metakaolinite phase ($Al_2O_3.2SiO_2$). The intensity for most peaks is also suppressed since other clay minerals partly decompose and free SiO_2 may be produced, leading to a sharper quartz peak at 26.67° in calcinated clay compared with the raw clay.

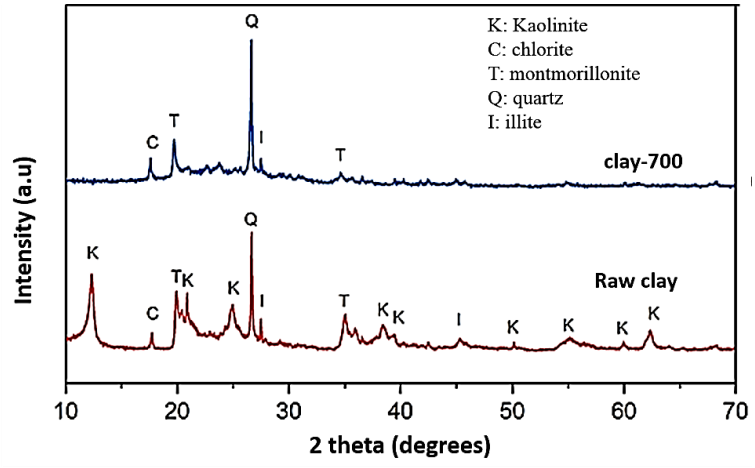

Figure 2. XRD patterns of raw clay and clay calcined at 700˚C

3.2. Activation of clay by acids

3.2.1. Color

The color of H_3PO_4 and H_2SO_4 solution during the activation was white and translucent, while that of HCl changed to yellow, as observed in Figure 3. The reactions of clay with HCl produce mainly aluminum chloride, which is white. However, iron impurity results in $FeCl_3$ which is light yellow.

In Figure 4, the color of raw clay is grayish white (Figure 4a) while that of calcinated clay is pinkish white (Figure 4b). Calcinated clay is more porous because of the loss of adsorbed and binding water, resulting in finer particles when ground. After being activated by acid, the clay became white as seen in Figure 4c because color ions like Fe^{3+}, Ti^{4+}, Mn^{2+} were almost removed from the solid composition.

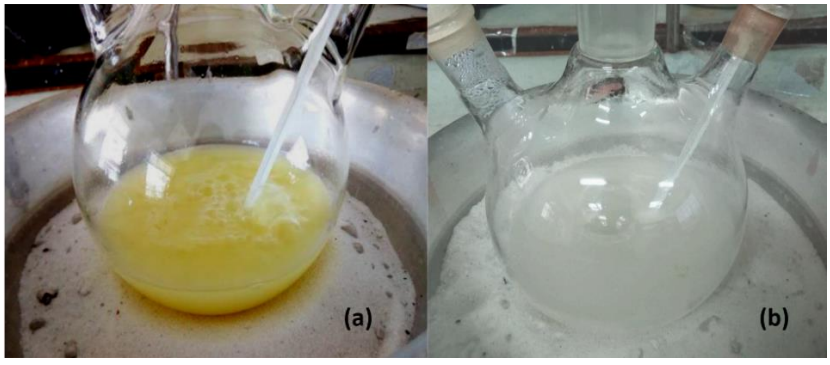

Figure 3. Color of acid solution during activation at 110˚C: (a) HCl and (b) H_3PO_4 and H_2SO_4

Figure 4. Color of clay samples: (a) raw clay, (b) calcinated clay at 700°C, and (c) activated clay by HCl

3.2.2. Weight loss after activation

Clay loses its weight in acids because clay minerals, which contain mainly SiO_2 and Al_2O_3, and other metal oxides react with acids to form free SiO_2 and soluble salts. Table 1 shows data on the weight loss after activation with different acids in 6, 12, and 18 h. A longer activation time results in more clay weight loss (Figure 5). However, with H_3PO_4 6 M, the weight loss increases negligible with a time longer than 6 h (from 39.75 to 40.25%), showing that the remaining solid after 6h activation was almost inactive in H_3PO_4. Therefore, with H_3PO_4 6 M solution, the activation time should not be longer than 6 h.

For HCl 6M, the weight loss is higher and rises slightly with time from 6 to 18 h activation, from 42.25% to 44.00%. Meanwhile, the activation with H_2SO_4 6M has the lowest weight loss at 6 h activation, with 34.50% compared to 39.25% (H_3PO_4) and 42.25% (HCl). The weight loss increases significantly with time and the dissolution seems to continue. Long activation time for H_2SO_4 is, therefore, a disadvantage. Panda et al. (2010) reported a shorter treatment time with H_2SO_4 (Panda et al., 2010). This may be because of the finer clay particles applied in their process.

Table 1. Weight loss of clay after activation by different acids

Acid	Activated time (h)	Initial weight (g)	Weight after activation (g)	Weight loss (g)	Weight loss (%)
HCl 6M	6	8.00	4.62	3.38	42.25
	12		4.56	3.44	43.00
	18		4.48	3.52	44.00
H_2SO_4 6M	6		5.24	2.76	34.50
	12		4.95	3.05	38.13
	18		4.60	3.40	42.50
H_3PO_4 6M	6		4.82	3.18	39.75
	12		4.80	3.20	40.00
	18		4.78	3.22	40.25

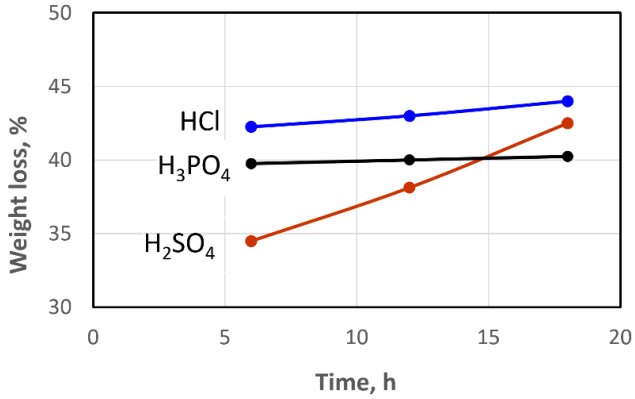

Figure 5. Time dependence of weight loss of the clay samples activated by H_3PO_4 6 M, H_2SO_4 6 M and HCl 6 M at 110°C

3.2.3. Effect of using H_3PO_4 for the activation at different times

Figure 6 illustrates XRD patterns of clay samples activated by H_3PO_4 6M solution in 6, 12, and 18 h compared to that of calcinated clay at 700°C. Chlorite and other minor minerals were almost dissolved by H_3PO_4 leaving mainly quartz (SiO_2) featured by 2θ at 20.88° and 26.66° and illite at 27.2°. The dissolution also resulted in increasing free crystalline SiO_2, observed by sharp peaks in activated samples. Longer activation times seem unnecessary since the XRD pattern of clay activated in 6 h has no distinction from those of samples activated in 12 and 18 h. H_3PO_4, a medium acid, cannot destroy the crystalline structure of quartz mineral despite high acid concentration and long reaction time.

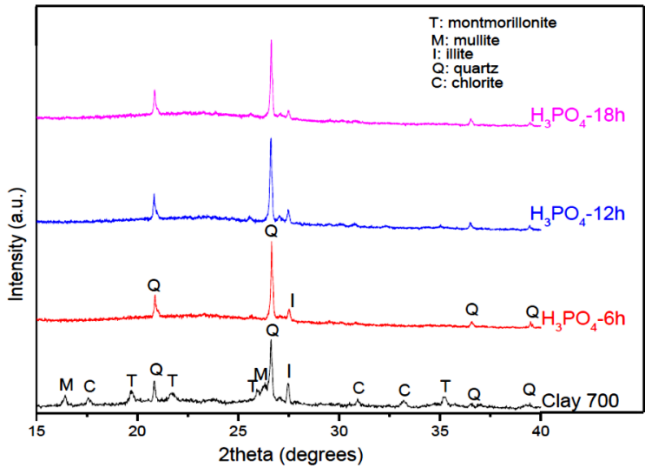

Figure 6. XRD patterns of clay samples activated by H_3PO_4 6 M in 6 h, 12 h and 18 h at 110°C

3.2.4. *Effect of using H_2SO_4 for the activation at different times*

The activation of clay by H_2SO_4 6 M was performed at 110°C over 6, 12 and 18 h. The structural changes were shown in XRD patterns (Figure 7). In 6h, except quartz and illite, other minerals were dissolved out, similar to the case using H_3PO_4. The characteristic peak for quartz at $2\theta = 26.67^{\circ}$ increases the intensity since more free SiO_2 is released because of the reaction of the minerals with acid, as for metakaolinite ($Al_2Si_2O_7$) described as follows

$$Al_2Si_2O_7 + 3H_2SO_4 \rightarrow Al_2(SO_4)_3 + 2SiO_2 + 3H_2O$$

However, when increasing reaction time to 12 h, the characteristic peak for illite at $\theta = 27.23^{\circ}$ disappears, i.e., it is completely dissolved. In addition, the quartz peak decreases intensity, meaning SiO_2 was partially dissolved, or the crystal structure of quartz was disordered by strong acid. This may lead to the formation of amorphous SiO_2 in the sample. A long reaction time of 18 h resulted in less crystalline SiO_2 in the sample with low intensity of quartz peak, although a significant amount of the solid particles was obtained. We might infer that the remaining SiO_2 solid particles contain a high ratio of amorphous silica.

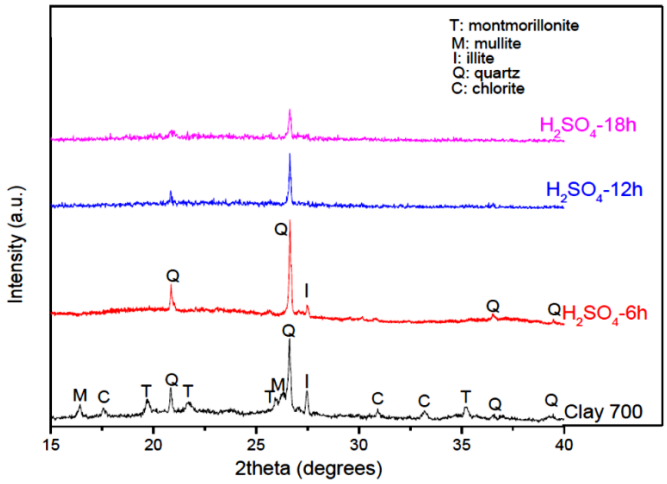

Figure 7. XRD patterns of clay samples activated by H_2SO_4 6 M in 6 h, 12 h and 18 h at 110°C

3.2.5. *Effect of using HCl for the activation at different times*

Figure 8 represents XRD patterns of clay samples activated by HCl at 110°C. After activation for 6 h, quartz is the major crystalline phase remaining. The crystallized SiO_2 phase reduces significantly for 12 h activation with low intensity of characteristic peak at 26.67° although the weight loss increases slightly (42.25% for 6 h and 43.00% for 12 h). This means that besides the dissolution of oxides like Al_2O_3

Fe_2O_3, MgO at the early stage, the crystalline SiO_2 phase transformed to amorphous when the activation process was prolonged. This is confirmed by as long a heating time as 18 h resulting in mainly amorphous silica observed in Figure 7. Therefore, it might be inferred that the surface area of activated clay by HCl would increase compared to that of clay activated by H_3PO_4 or H_2SO_4, where crystalline silica is still maintained. This would be discussed further in section 3.5.

The activation with all three acids leads to weight loss between 40-45 wt% resulting from the reaction of metal oxides with acid. H_3PO_4, a medium-strong acid, activates clay but the crystalline phase remains significant after 18 h reaction. With H_2SO_4, the crystal structure of clay was destroyed and little crystalline SiO_2 (quartz) was observed when activation after 18 h. The activation with HCl after 18 h leads to amorphous silica composed in the sample. Therefore, if the amorphous phase is needed, then the activation with HCl is recommended. For this reason, the clay activated with HCl was used for further investigation.

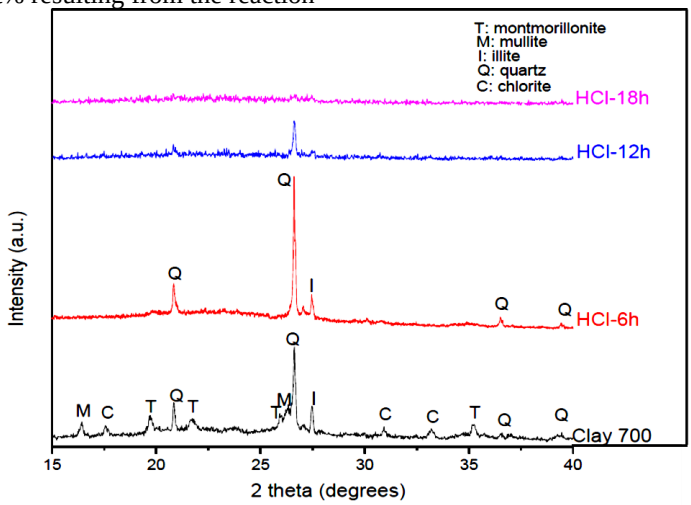

Figure 8. XRD patterns of clay samples activated by HCl 6M in 6 h, 12 h, and 18 h at 110°C

3.3. Chemical composition of clay

Table 2 shows the chemical composition of raw ball clay and activated clay by HCl calculated from XRF analysis. Raw clay contains mainly Al_2O_3 (24.89 wt%) and SiO_2 (72.1 wt%), in which the molar ratio of SiO_2/Al_2O_3 = 4.9, showing that raw clay may be composed of kaolinite (SiO_2/Al_2O_3=2), montmorillonite (SiO_2/Al_2O_3 = 4) and a significant amount of free quartz (SiO_2). Other oxides were also found in clay with minor amounts. The small amount of Fe_2O_3 (0.12%) is relevant for the white color of this ball clay.

After activation, the sample contains mainly SiO_2 (97.1%), a small amount of Al_2O_3 (2.07%) and K_2O (0.77%). Compared to raw clay, the percentages of Al_2O_3 and other metal oxides reduce a great deal because of their reaction with strong acid resulting in soluble salts. This leads to an increase in silica percentage from 72.1% in raw clay to 97.1% in HCl-activated clay. SiO_2 is less reactive in acid than other metal oxides because it is amphoteric, thus, a great amount of SiO_2 remains in the final solid obtained. In raw ball clay, SiO_2 occurs as clay minerals, i.e., layer structured crystal lattice with tetrahedra of SiO_4 partially replaced by AlO_4, and free metal ions like Na^+, K^+, Ca^{2+}, Mg^{2+} randomly distributed in the structure. These free metal ions are prone to acid and easy to react, leaving the solid crystal structure with an unbalanced electrical charge. The layered structure is then destroyed when the Al ions of AlO_4 tetrahedra in the structure react with strong acids (Belver et al., 2002; Motlagh et al., 2011). From XRD patterns, it can be concluded that most SiO_2 remained after activation occurs in gel form, which on drying, becomes amorphous silica powder, especially in activated clay with HCl in 18 h, as observed in Figure 8.

Table 2. Chemical composition (wt%) of raw ball clay and activated clay by HCl calculated from XRF data

Composition	SiO_2	Al_2O_3	K_2O	MgO	Fe_2O_3	TiO_2	MnO	CaO	Rb_2O_3	Y_2O_3	Others
Raw ball clay (wt%)	72.1	24.89	2.132	0.549	0.119	0.013	0.027	0.092	0.024	0.009	0.029
Activated clay (wt%)	97.1	2.068	0.765	-	0.017	0.005	-	0.025	0.005	-	0.009

3.4. FTIR

Figure 9 illustrates the FTIR spectra of clay samples in which changes of bonding nature before and after treatment are revealed. A summary of the important FTIR band assignments is reported in Table 3. Raw clay shows peaks at 3445 cm^{-1} and 1634 cm^{-1} assigned to the adsorbed water and bending H-O-H, respectively, in the samples compared to no peak observed in calcinated clay. This peak was again observed in acid-treated samples since they were activated in an aqueous acid solution. According to XRF analysis (Table 2), the changes in the compositions occur mainly because of the structural destruction at Al octahedral sites in strong acid solution to become solvable products, resulting in silica powder with little Al component left.

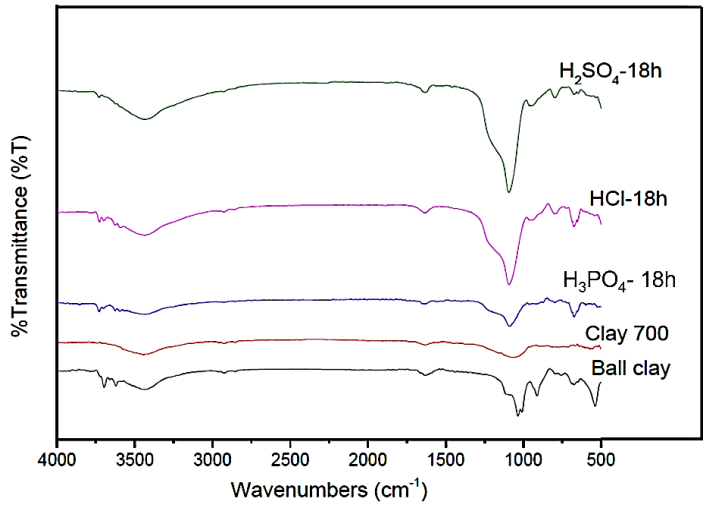

Figure 9. FTIR curves of raw ball clay, calcinated clay at 700˚C and activated clays with H_3PO_4 6 M, HCl 6 M, and H_2SO_4 6 M at 110˚C in 18 h

Table 3. Summary of bonding assignments from FTIR bands of clay samples (Davarcioglu & Ciftci, 2010; Panda et al., 2010)

Band (cm^{-1})					
Raw clay	Calcinated clay at 700˚C	Activated clays			Assignments
		H_3PO_4-18 h	HCl-18 h	H_2SO_4-18 h	
3698	-	3725	3725	3725	Al-O-$H_{stretching}$
3662	-	-	-	-	Al-O-$H_{stretching}$
3625	-	-	-	-	Al-O-$H_{stretching}$
3445	3445	3445	3445	3445	-OH from absorbed water
1634	1634	1634	1634	1634	H-O-$H_{bending}$
1116	1120	-	-	-	Si-$O_{stretching}$
1026	1026	1026	1026	1026	Si-$O_{stretching}$
1006	-	-	-	-	Si-$O_{stretching}$
922	-	924	927	952	Al-Al-OH
-	-	796	796	796	Free SiO_2 /quartz admixture
755	-	-	-	-	Si-O-Al
685	685	685	685	685	Si-O out of plane bending
537	542	-	-	-	Si-O-$Al_{bending}$

The FTIR spectroscopy also shows clearly that typical peaks of clay minerals including the stretching Al-O-H in the range of 3662 to 3625 cm^{-1}, the stretching Si-O (at 1116, 1026 cm^{-1}), and the Si-O-Al (755 cm^{-1}) disappear, and only minor stretching Al-O-H peak left at 3725 cm^{-1} after acid activation. Another peak for stretching Si-O at 1026 cm^{-1}, however, becomes stronger with acid activation. This peak relates to the Si-O in the tetrahedral in silica, while others relate to Si-O in the sheet structure of clay minerals, which are destroyed in acid (Panda et al, 2010). A new peak at 796 cm^{-1} in activated samples was assigned to the formation of free amorphous SiO_2 and quartz admixture, which agrees with XRF analysis and XRD patterns of this study, showing the characteristic peak of SiO_2 (at 2 theta 26.67°) but with low intensity. These results are in accordance with previous reports (Mako et al., 2006; Bendou & Amrani, 2014; Edama et al, 2014).

3.5. BET

Table 4 provides data on the specific surface area (S_{BET}) of several types of clay before and after the activation by HCl at different conditions. They all have a typically low surface area as reported (Castelano, 2010; Edama et al., 2013). Edama et al. (2013) showed the S_{BET} of Sayong kaolinite clay increased from 24.46 $m^2.g^{-1}$ to 64.04 $m^2.g^{-1}$ when it was activated in 4 h, 100°C by HCl 5 M. The increase is small compared to that of activated Spanish kaolin (from 18 to 219 $m^2.g^{-1}$) when the process was performed in 24 h, 90°C in HCl 6 M (Belver et al., 2003). The S_{BET} of Truc Thon ball clay in this work increases significantly from 10.55 $m^2.g^{-1}$ to 178.53 $m^2.g^{-1}$ after the activation in HCl 6 M, 18 h at 110°C, which is comparable to Cretacean kaolinferous clay activated also in HCl 6 M, 90°C in only 3 h with refluxing condition (San Cristóbal et al., 2009). It is noticeable that the activation time and acid concentration play an important role in reducing the particle size of clay. Applying the refluxing condition can help to decrease the reaction time by avoiding water loss which leads to the drying of the suspension. In all cases, the acid activation is remarkably effective in increasing the surface area of clay, which is good preparation for clay to be used as an adsorbent.

Table 4. Specific surface area of several types of clay

Types of clay	Specific surface area ($m^2.g^{-1}$)		Activation condition	Study
	Inactivated clay	Activated clay		
Sayong kaolinite clay	24.46	64.04	HCl 5 M, 100°C, 4 h	Edama et al. (2013)
Spanish kaolin	18	219	HCl 6 M, 90°C, 24 h	Belver et al. (2002)
Cretacean kaolinferous clay	14	189	HCl 6 M, 90°C, 3 h, refluxing	San Cristóbal et al. (2009)
Truc Thon ball clay	10.55	178.53	HCl 6 M, 110°C, 18 h, refluxing	This study

3.6. Surface charge of clay

Figure 10 illustrates the dependence of ΔpH ($\Delta pH = \Delta pH_{final} - \Delta pH_{initial}$) on initial pH, through which the point of zero charge (pH_{pzc}) of clays can be determined as the interception point at ΔpH = 0. The pH_{pzc} of inactivated and calcinated clays are 6.4 and 6.7, respectively. Slightly higher pH_{pzc} of calcinated clay compared to that of inactivated clay results from the loss of physicowater in clay during calcination (Fumba et al., 2014). This shows that the untreated clay and thermally treated clay act as adsorbents with a negative surface charge in solutions at neutral and base media.

The HCl activation helps to move the pH_{pzc} to a much lower value, at pH 4. This is because the acid-activated clay contains little exchangeable cations on the surface due to the dissolution of metal cations in the clay structure. Instead, the proton H^+ may attach to the surface and the pores of the activated clay leading to the lowering of pH when dispersed in the solution compared to untreated clay (Teng & Lin, 2006).

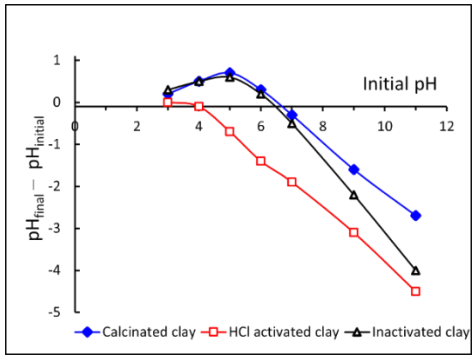

Figure 10. Dependence of ΔpH (= $pH_{final} - pH_{initial}$) on initial pH of inactivated clay, calcinated clay and HCl activated clay

3.7. SEM

FE-SEM micrographs of the calcinated and activated clays are shown in Figure 11. Aggregates are observed, in which plates and flaky particles are typical for clay samples. However, the morphology of activated clay (Figure 11b) looks more porous and spongier than that of calcinated clay (Figure 11a). This results in a much higher surface area for activated clay as measured and discussed above. Moreover, Figure 11b shows that the clay particles are well-bonded into agglomerates rather than separate grains as observed in Figure 11a. This agrees with other reports (Panda et al., 2010; Emada et al., 2013).

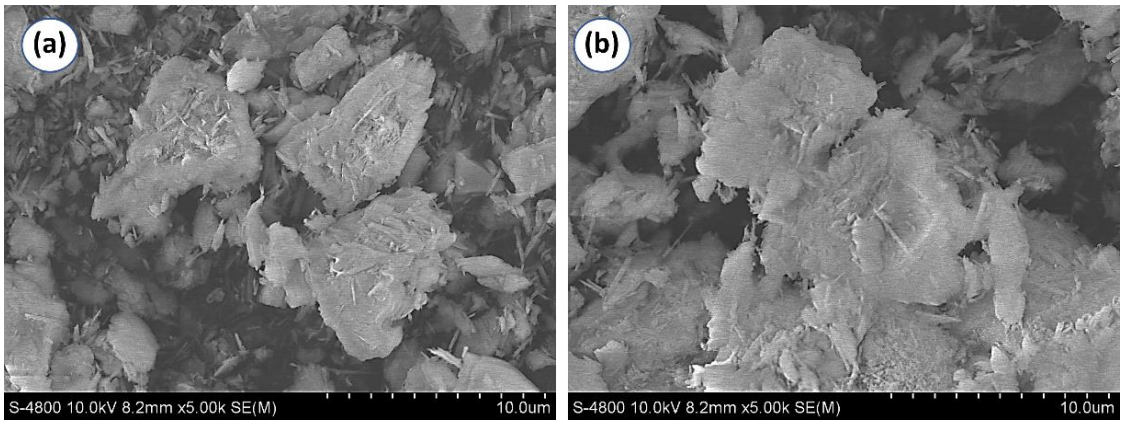

Figure 11. Field emission scanning electron micrograph of calcinated clay at 700˚C (a) and activated clay at 110˚C, 18 h in HCl 6 M (b) at a magnification of 5000x

4. CONCLUSION

This study provides information on the acid activation process of Truc Thon ball clay, in which the acid at a fixed concentration of 6 M played an important role in changing the clay structure gradually from crystalline to amorphous, especially with HCl. This process was also accompanied by the dissolution of metal oxides into the acid solution, resulting in the decline of metal components in the clay, hence, the percentage of SiO_2 increased. The activated clay has a much higher surface area compared to that of raw clay, which is promising to be applied in adsorption techniques for air and wastewater treatment. It is also suitable for use as a catalyst with some modifications. Further research on using the activated clay in this study for the treatment of color or heavy metals in the wastewater is therefore necessary for proving the effectiveness of acid-treated clay as adsorbents.

ACKNOWLEDGMENT

The authors acknowledge Can Tho University for funding this research under project grant T2021-11.

REFERENCES

Ahmadi, A., Foroutan, R., Esmaeili, H., & Tamjidi, S. (2020). The role of bentonite clay and bentonite clay@$MnFe_2O_4$ composite and their physicochemical properties on the removal of Cr(III) and Cr(VI) from aqueous media. *Environmental Science and Pollution Research*, *27*, 14044–14057. https://doi.org/10.1007/s11356-020-07756-x

Akpomie, K. G. & Dawodu, F. A. (2016). Acid-modified montmorillonite for sorption of heavy metals from automobile effluent. *Beni-Suef University Journal of Basic and Applied Sciences*, *5*(1), 1–12. https://doi.org/10.1016/j.bjbas.2016.01.003

AlKhafaji, K. S., Al-Zaidi, B. Y., Shakor, Z. M., & Hussein, S. J. (2022). Comparison between Conventional and Metakaolin bi-functional Catalyst in the Hydrodesulfurization Operation. *Journal of Petroleum Research and Studies*, *12*(2), 64-80. https://doi.org/10.52716/jprs.v12i2.658

Belver, C., Muñoz, A., & Vicente, M. A. (2002). Chemical activation of a kaolinite under acid and alkaline conditions. *Chemistry of Materials*, *14*(5), 2033-2043. https://doi.org/10.1021/cm0111736

Bendou, S. & Amrani, M., (2014). Effect of Hydrochloric Acid on the Structural of Sodic-Bentonite Clay. *Journal of Minerals and Materials Characterization and Engineering*, *2*(5), 404-413. http://dx.doi.org/10.4236/jmmce.2014.25045

Bhattacharyya, K. G., & Gupta, S. S. (2006). Pb(II) uptake by kaolinite and montmorillonite in aqueous medium: Influence of acid activation of the clays,

Colloids and Surfaces A: Physicochemical and Engineering Aspects, *277*(1-3), 191-200. https://doi.org/10.1016/j.colsurfa.2005.11.060

Castelano, M., Turturro, A., Riani, P., Montanari, T., Finocchio, E., Ramis, G., & Busca, G. (2010). Bulk and surface properties of commercial kaolins. *Applied Clay Science*, *48*, 446-454. http://dx.doi.org/10.1016/j.clay.2010.02.002

Crundwell, F. K. (2014). The mechanism of dissolution of minerals in acidic and alkaline solutions: Part II Application of a new theory to silicates, aluminosilicates and quartz, *Hydrometallurgy*, *149*, 265–275. https://doi.org/10.1016/j.hydromet.2014.07.003

David, M. K., Okoro, U. C., Akpomie, K. G., Okey C., & Oluwasola, H. O. (2020). Thermal and hydrothermal alkaline modification of kaolin for the adsorptive removal of lead(II) ions from aqueous solution. *SN Applied Sciences*, *2*(1134). https://doi.org/10.1007/s42452-020-2621-7

Davarcioglu, B., & Ciftci, E. (2010). The clay minerals observed in the building stones of Aksaray-Guzelyurt area (Central Anatolia-Turkey) and their effects. *International Journal of Physical Science*, *5*(11), 1734-1743. https://doi.org/10.5897/IJPS.9000549

Dim, P. E., & Termtanun, M. (2021). Treated clay mineral as adsorbent for the removal of heavy metals from aqueous solution. *Applied Science and Engineering Progress.* https://doi.org/10.14416/j.asep.2021.04.002

Edama, N. A., Sulaiman, A., Ku Hamid, K. H., Mohd Rodhi, M. N., Mohibah, M., & Abd Rahim, S. N. (2013). The Effect of Hydrochloric Acid on the Surface Area, Morphology and Physico-Chemical Properties of Sayong Kaolinite Clay. *In Key Engineering Materials 594–595*, 49–56. Trans Tech Publications, Ltd. https://doi.org/10.4028/www.scientific.net/kem.594-595.49

Fumba, G., Essomba, J. S., Tagne, G. M., Nsami, N. J., Désiré, P., Bélibi P. D. B., & Mbadcam, J. K. (2014). Equilibrium and Kinetic Adsorption Studies of Methyl Orange from Aqueous Solutions Using Kaolinite, Metakaolinite and Activated Geopolymer as Low Cost Adsorbents. *Journal of Academia and Industrial Research*, *3*(4), 156-163. https://doi.org/10.1016/j.materresbull.2009.07.016

Komadel P., & Madejová J. (2013). Chapter 10.1 Acid activation of clay minerals, *Developments in clay science*, *5*, 385-409. https://doi.org/10.1016/B978-0-08-098258-8.00013-4

Mako, E., Senkar, Z., Kristof, J., & Vagvolgyi, V. (2006). Surface modification of mechanochemically activated kaolinites by selective leaching. *Journal of Colloid and Interface Science*, *294*, 362-370. http://dx.doi.org/10.1016/j.jcis.2005.07.033

Motlagh, K., Youzbashi, A. A., & Rigi, Z. A. (2011). Effect of Acid Activation on Structural and Bleaching Properties of a Bentonite. *Iranian Journal of Material Science and Engineering*, *8*(4), 50-56.

Murray, H. H. (2006). Chapter 2 Structure and Composition of the Clay Minerals and their Physical and Chemical Properties. *Developments in clay science*, *2*, 7-31. https://doi.org/10.1016/S1572-4352(06)02002-2

Ndé, H. S., Tamfuh, P. A., Clet, G., Vieillard, J., Mbognou, M. T., & Woumfo, E. D. (2019). Comparison of HCl and H_2SO_4 for the acid activation of a cameroonian smectite soil clay: palm oil discoloration and landfill leachate treatment, *Heliyon*, *5*(12), e02926. https://doi.org/10.1016/j.heliyon.2019.e02926

Panda, A. K., Mishra, B. G., Mishra, D. K., & Singh R. K. (2010). Mineralogical, crystallographic and morphological characteristics of natural kaolins from the Ivory Coast (West Africa), *Colloids and Surfaces: A Physicochemical Engineering Aspects 363*, 98-104 https://doi.org/10.1016/j.colsurfa.2010.04.022

Parker, W. O., & Kiricsi, I. (1995). Aluminum complexes in partially hydrolyzed aqueous $AlCl_3$ solutions used to prepare pillared clay catalysts, *Applied Catalysis A: General*, *121*(1), L7-L11. https://doi.org/10.1016/j.colsurfa.2005.11.060

San Cristóbal, A. G., Castelló R., Luengo M. A. M., & Vizcayno, C. (2009). Acid activation of mechanically and thermally modified kaolins. *Materials Research Bulletin*, *44*(11), 2103–2111. https://doi.org/10.1016/j.materresbull.2009.07.016

Teng, M. Y. & Lin, S. H. (2006). Removal of methyl orange dye from water onto raw and acid activated montmorillonite in fixed beds. *Desalination*, *201*(1-3), 71-81. https://doi.org/10.1016/j.desal.2006.03.521